

Strong correlations between power-law growth of COVID-19 in four continents and the inefficiency of soft quarantine strategies

Cesar Manchein^{1,*}, Eduardo L. Brugnago^{2,†}, Rafael M. da Silva^{2,‡}, Carlos F.O. Mendes^{3,§} and Marcus W. Beims^{2,¶}

¹Departamento de Física, Universidade do Estado de Santa Catarina, 89219-710 Joinville, SC, Brazil

²Departamento de Física, Universidade Federal do Paraná, 81531-980 Curitiba, PR, Brazil and

³ Escola Normal Superior, Universidade do Estado do Amazonas, 69050-010 Manaus, AM, Brazil

(Dated: January 15, 2022)

In this work we analyse the growth of the cumulative number of confirmed infected cases by the COVID-19 until March 27th, 2020, from countries of Asia, Europe, North and South America. Our results show (i) that power-law growth is observed for all countries; (ii) that the distance correlation of the power-law curves between countries are statistically highly correlated, showing the universality of such curves around the World; and (iii) that soft quarantine strategies are inefficient to flatten the growth curves. Furthermore, we present a model and strategies which allow the government to reach the flattening in the power-law curves. We found that, besides the social isolation of individuals, of well known relevance, the strategy of *identifying* and *isolating* infected individuals could be of more relevance to flatten the power-laws. These are essentially the strategies used in the Republic of Korea. In fact, our results suggest that the allowed *balance* between social isolation and degrees of isolation of infected individuals can be used to prevent economic catastrophes. The high correlation between the power-law curves of different countries strongly suggest that the government containment measures can be applied with success around the whole World. These measures must be scathing and applied as soon as possible.

PACS numbers: Pacs: 87.19.xd, 05.45.Tp, 87.18.-h

Since the identification of a novel coronavirus (COVID-19) in Wuhan, China, in December 2019, the virus kept spreading around the World. One of the most remarkable characteristics of COVID-19 is its high infectivity, resulting in a global pandemic. In this complex scenario, tasks like protect the people from the infection and the global economy may be considered two of the greater challenges nowadays. In order to improve our knowledge about the COVID-19 and its behavior in different countries over the World, we exhaustively explore the real time-series of cumulative number of the confirmed infected cases by the COVID-19 in the last months until March 27th, 2020. In our analysis we considered countries of Asia, Europe, North and South America. Our main findings clearly show the existence of a well established power-law growth and a strong correlation between power-law curves obtained for different countries. These two observations strongly suggest an universal behavior of such curves around the World. To improve our analysis, we use a model with six autonomous ordinary differential equations, based on the well-known SEIR (Susceptible-Exposed-Infectious-Recovered) epidemic model (considering quarantine procedures) to propose efficient

strategies which allow the government to increase the flattening of the power-law curves. Additionally, we also show that soft measures of quarantine are inefficient to flatten the growths curves.

I. INTRODUCTION

The astonishing increase of positively diagnosed cases due to COVID-19 has called the attention of the whole World, including researchers of many areas and governments. It urges [1] to find explanations for the already known data and models which may allow us to better understand the evolution of the viruses. Such explanations and models can hopefully be used to implement social policies and procedures to decrease the number of infections and deaths. Time urges to avoid economic and social catastrophes.

In general, the average reproductive number R_0 , which gives the number of secondary infected individuals generated by a primary infected individual, is the key quantity which determines the dynamical evolution of the epidemic [2]. Usually, for values $R_0 < 1$, the number of new infected individuals decreases exponentially. For $1 < R_0 < \infty$ this number increases exponentially [2, 3]. However, nature is full of surprises and there are plenty of cases for which the exponential behavior is substituted by power-law [4] and are related to branching processes with diverging reproductive number [2], scale free networks and small worlds [5]. It was already suggested in the literature that the COVID-19 growth might be a small world [6]. This is in agreement with recent results [7] suggesting that for many countries around the World

* cesar.manchein@udesc.br

† elb@fisica.ufpr.br

‡ rmarques@fisica.ufpr.br

§ cfabio.mendes@gmail.com

¶ mbeims@fisica.ufpr.br

the COVID-19 growth has the tendency to follow the power-law.

In fact, recent analysis regarding the behavior of the COVID-19 in China demonstrated a power-law t^μ growth of infected cases [8]. Authors found exponents around $\mu = 2.1 \pm 0.3$, which do not vary very much for different provinces in China. This suggests that socio-economical differences, local geography, differences in containment strategies, and heterogeneities essentially affect the *value* of the exponent μ , but not the qualitative behavior. A model of coupled differential equations, which includes quarantine and isolations effects, was used by the authors to match real data. Power-law growths for China were obtained also in another study and a possible relation to fractal kinetics and graph theory is discussed [9].

In line to the above last week publications, the present work analyzes the time-series evolution of the COVID-19 for the following countries: Brazil, China, France, Germany, Italy, Japan, Republic of Korea, Spain, and United States of America (USA). In all cases we observe a power-law increase for the positive detected individuals, where the exponent μ changes for different countries. In addition to the power-law behavior we also computed the Distance Correlation (DC) [10] between pairs of countries. The DC is able to detect nonlinear correlations between data [11, 12]. We show that power-law data are highly correlated between all analyzed countries. This strongly suggest that governmental strategies to flatten the power-law growth, valid for one country, can be successfully applied to other countries and continents. Furthermore, a model of Ordinary Differential Equations (ODEs) is proposed and some strategies to flatten the power-law curves are discussed using the numerical simulations.

The paper is divided as follows. Section II presents the power-law growth of confirmed infected cases of COVID-19 and the DC between pairs of countries is determined. Section III discusses numerical results using the proposed model showing many strategies to flatten the power-law growth. In Section IV we summarize our results.

II. REAL DATA ANALYSIS

A. Power-law growths

Figure 1 displays data of the cumulative number of confirmed positive infected cases by COVID-19 of nine countries as a function of the days. The analyzed countries are (in alphabetic order): Brazil, China, France, Germany, Italy, Japan, Republic of Korea, Spain, and USA. Data were collected from the situation reports pub-

lished daily by the World Health Organization (WHO) [13]. We notice that the values in the vertical axis in Fig. 1 change for different countries. Initial data regarding the incubation time were discarded since they do not contribute to the essential results discussed here. Black-continuous curves are the corresponding fitting curves $\alpha + \beta t^\mu$, where t is the time given in days, α , β , and μ are parameters. The insets in all plots show the data in the log-log scale. Straight lines in the log-log plot represent power-law growth. The fact that the growth increases as a power-law is good news since it increases slower than the exponential one. However, that is not good enough.

The regimes with power-law growth are the most relevant to be discussed since they provide essential information of what is expected for the future and possible attitudes needed to flatten the curves. The exponent μ changes for distinct countries and the complete fitting parameters are given in Table I. Results in Table I are presented in decreasing order of the exponent μ . USA [Fig. 1(a)] has by far the largest exponent and therefore became already the country with epidemic records. Even though Germany [Fig. 1(b)] reported a small number of deaths, it has the second large exponent, followed by Spain [Fig. 1(c)], France [Fig. 1(d)] and Italy [Fig. 1(e)], in this order. China [Fig. 1(f)], Brazil [Fig. 1(g)], Japan [Fig. 1(h)], and Republic of Korea [Fig. 1(i)], in this order, are the last in the list. In the case of China and Republic of Korea the power-laws are more clear due to the number of available data. For these two countries a flatten is observed after the power-law. The jump observed after 30 days in China data are due to a change in the counting procedure of infected cases (see the situation report on February 17th, 2020, in Ref. [13]). Republic of Korea, on the other hand, focused on identifying infected patients immediately and isolating them to interrupt transmission [14]. It is interesting to note that for Japan, another country that adopted similar measures, we obtained a similar value for μ .

Table I. Details about the parameters of the fitting curves for the power-law behavior $\alpha + \beta t^\mu$ shown in Fig. 1.

Country	α	β	μ
USA	0	0.009	4.994 ± 0.216
Germany	0	0.223	3.734 ± 0.107
Spain	308	0.386	3.686 ± 0.037
France	280	0.467	3.341 ± 0.031
Italy	0	2.868	2.934 ± 0.040
China	98	24.013	2.492 ± 0.020
Brazil	59	18.450	1.971 ± 0.054
Japan	112	3.107	1.685 ± 0.034
Republic of Korea	0	62.574	1.670 ± 0.065

The most desired behavior is that the exponent μ be-

comes smaller leading to a flattening of the curves. But

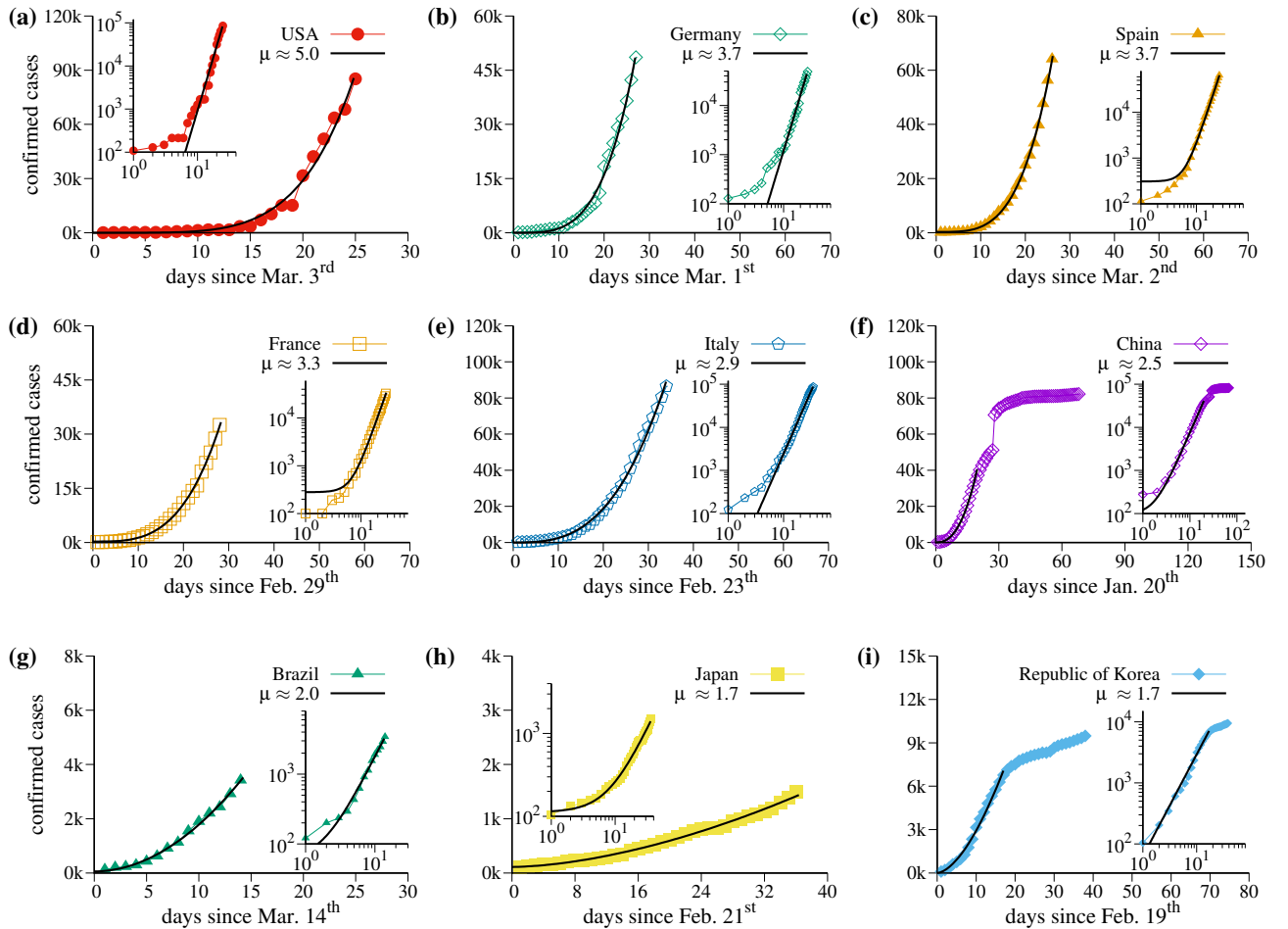


Figure 1. Cumulative number of confirmed infected cases by COVID-19 as a function of time for all countries studied in this work, excluding days with less than 100 infected. The black-continuous curves represent the function $\alpha + \beta t^\mu$ that fit the time-series, and the parameters α , β , and μ for each country are described in Table I.

this is apparently not that easy. Besides USA and Germany, which have a distinct inclination in the beginning of their power-laws, and China and Republic of Korea, which are stabilizing the epidemic spread, for all other countries the growth remains strictly on the fitted curve and μ essentially does not change in time. In Sec. III we discuss some possibilities to flatten the power-laws.

B. Distance Correlation between countries

The power-law observed in all cases from Fig. 1 are certainly not a coincidence, but a consequence of virus propagation in scale free systems. To quantify the relation between the power-law growth we use the DC, which is a statistical measure of dependence between random vectors [10, 15–18]. Please do not confuse the word distance with the geographical distance between the analyzed countries. The most relevant characteristics of DC is that it will be zero if and only if the data are independent and equal to one for maximal correlation between

data. Details about the definition of DC are given in Sec. V.

Figure 2 presents specific results for the DC calculated between some selected countries, namely Brazil, Italy, Japan, and USA. Italy were chosen due to their relevance in Europe, relevance regarding to typical data of the virus. USA was chosen for being nowadays the top affected country and Brazil and Japan representing distinct continents and distinct epidemic containment measures. Thus, we compute the DC between four continents. Figures 2(a), 2(b), 2(c), 2(g), 2(h), and 2(i) are the cumulative number of confirmed cases in each country, as in Fig. 1, but considering data since the first day the infections were reported. In these curves we clearly see the initial plateaus due to the incubation time. After the plateaus, a qualitative change to a power-law growth (the same from Fig. 1) occurs. The time for which the qualitative change occurs is distinct for each country.

Figures 2(d), 2(e), 2(f), 2(j), 2(k), and 2(l) display the corresponding DC calculated between the countries. Results show that DC between the curves is relatively high

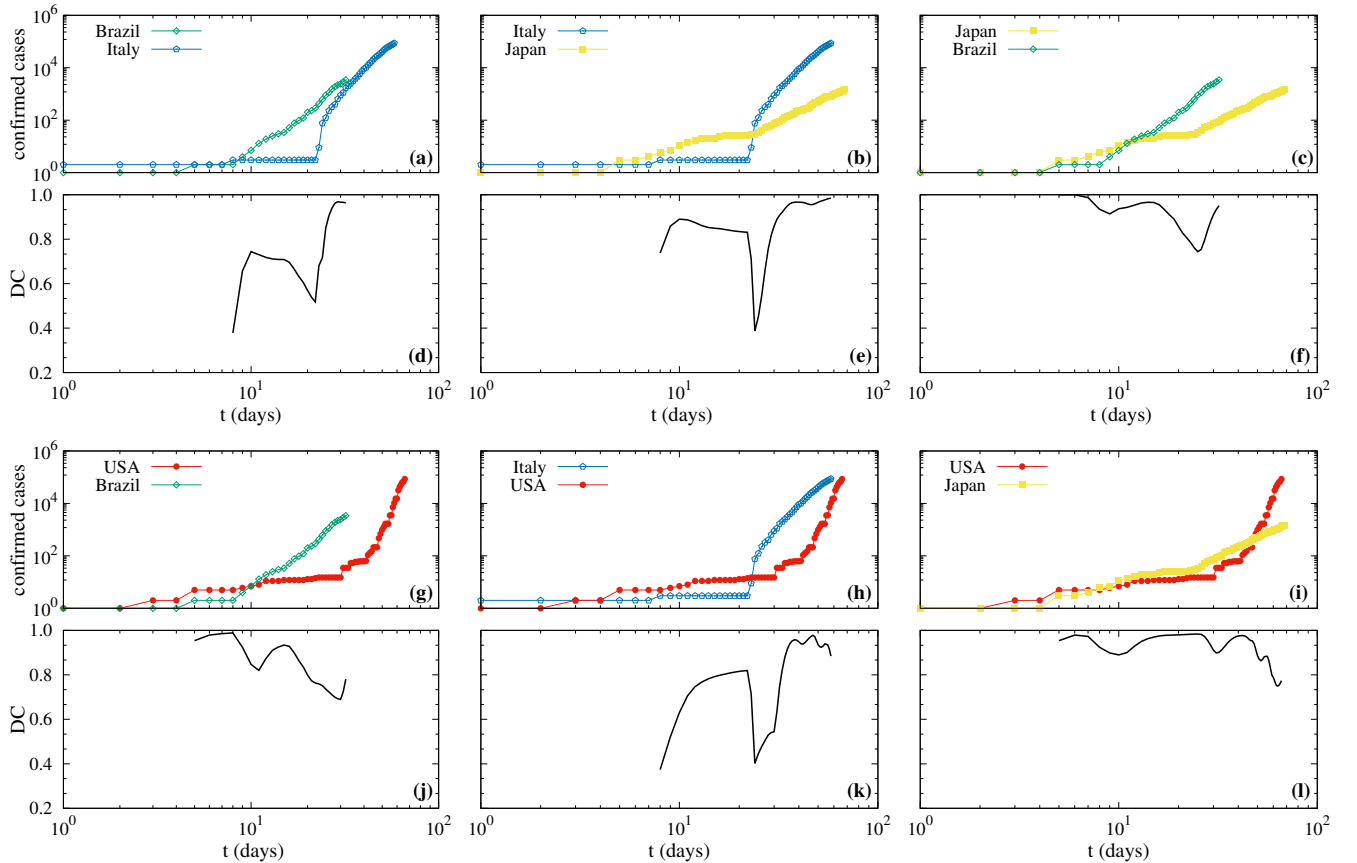


Figure 2. In panels (a), (b), (c), (g), (h), and (i) the log-log plot of the cumulative numbers of confirmed infected cases as a function of time are presented for the possible pairs of countries formed between Brazil, Italy, Japan, and USA. The semi-log plot of DC calculated between these pairs of countries is presented in panels (d), (e), (f), (j), (k), and (l), respectively.

in the beginning. The lowest values are obtained for the DC between Brazil and Italy, in Fig. 2(d), and for the DC between Italy and USA, shown in Fig. 2(k), both cases around $DC = 0.4$. The DC decays substantially when the power-law starts in one country but not in the other. The exception is between Japan and USA. After some days, when both countries reach the power-law behavior, the values of DC become very close to 1. Thus,

they are *highly* correlated besides distinct exponents μ . Furthermore, the DC is not necessarily related to the exponent μ . One example can be mentioned. Even though USA has the largest exponent and Japan the lowest one (considering the error in Table I), they are highly correlated. Besides that, even though there are not many data available for Brazil, it seems to become more and more correlated with Italy and Japan.

III. PREDICTIONS AND STRATEGIES

The model proposed in this work for the numerical prediction and strategies is presented in details in Sec. VI. It is a variation of the well known Susceptible-Exposed-Infectious-Recovered (SEIR) epidemic model [19, 20] to propose efficient strategies which allow the government to increase the flattening in the power-law curves. Our SEIR model takes into account the isolation of infected individuals [21, 22]. In this case, the quarantine means the identification and isolation of infected individuals. The parameters are divided in two categories: (i) those

related to the characteristic of the virus spreading, defined *a priori* from other studies and (ii) those related to adjusting the model to the real data. These parameters can change according to social actions and governmental strategies.

Numerical results of this section take into account possible interferences or strategies from the government of each country, what means that some parameters must be changed after the last day of the real data. For each distinct strategy, we use distinct colors which are then plotted. The colors of the subtitles represent the application of distinct strategies which leads to distinct *scenarios*.

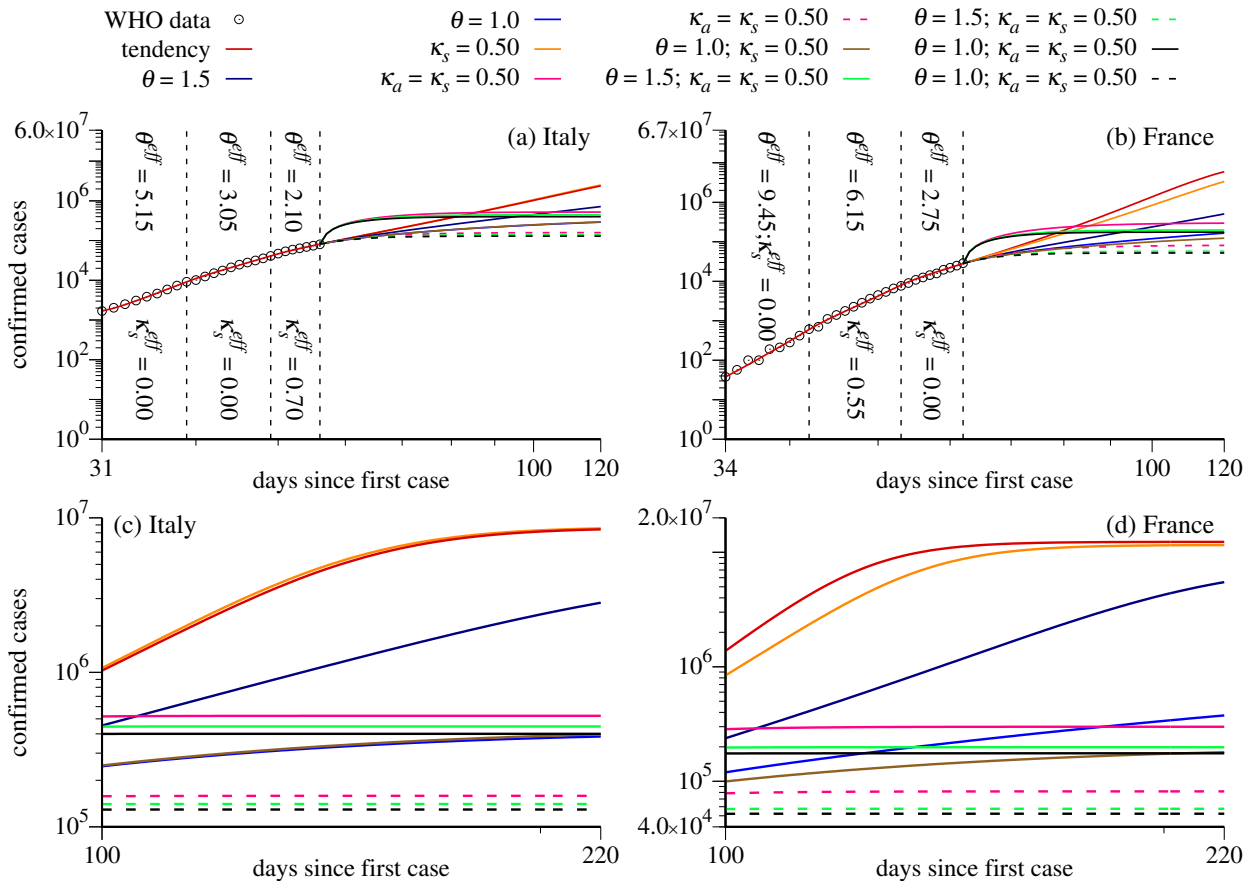


Figure 3. Log-log plot of cumulative number of confirmed cases (black circles) for Italy [(a) and (c)] and France [(b) and (d)] as a function of time and the projected number of cases (colored lines) using distinct governmental strategies (discussed in the text).

For a detailed explanation of variables and parameters,

please see the Sec. VI. The colors for the distinct scenarios are the following (for continuous curves):

- **Red curves:** the tendency which follows from the behavior of the last points of real data (last values for θ^{eff} and κ_s^{eff}). This is what happens if we do not applied strategies on March 28th.
- **Orange curves:** refers to the identification and isolation of individuals which manifest the symptoms. Here we use $\kappa_s = 0.50$, meaning the duration of one day of individuals of the group I_s before they are relocated to group Q .
- **Blue curves:** reduction of social interactions by using smaller values of θ . Dark blue for $\theta = 1.5$ and light blue for $\theta = 1.0$.
- **Magenta curves:** public action using test to identify the infected individuals in the population, in-

cluding symptomatic and asymptomatic individuals ($\kappa_s = \kappa_a = 0.50$).

- **Brown curves:** reduction of social interaction with $\theta = 1.0$ and isolation of the symptomatic individuals with $\kappa_s = 0.50$.
- **Light green curves:** reduction of social interaction together with tests to identify and isolate infected individuals. Here we use $\theta = 1.5$ and $\kappa_s = \kappa_a = 0.50$.
- **Black curves:** same as the light green curve but for $\theta = 1.0$ and $\kappa_s = \kappa_a = 0.50$.

For the dashed curves the configurations are the same inside each color. However, in these curves, the asymptomatic individuals are not accounted for. We notice

that without the realization of tests in the population, the asymptomatic individuals would not be computed.

We start discussing the cases of Italy and France, shown in Figs. 3(a), 3(c) and Figs. 3(b), 3(d), respectively. Figures 3(c) and 3(d) are the asymptotic predictions. The vertical axis is the cumulative number of positive infected individuals in the population. In the horizontal axis we have the days since the first computed case in these countries. Black circles are the real data starting from the power-law-like behavior discussed in Sec. II. During the times for which real data are available, the model chooses the values of the parameters θ and κ_s that better adjust the simulation results with the data. In the cases shown in Fig. 3 we needed three values of θ and κ_s , namely the values θ^{eff} and κ_s^{eff} given in the figures. As a consequence, the red curves are in full agreement with the data in this time interval. When the available data end, the simulation continues and the red curves can be used to predict the asymptotic number of confirmed cases since they represent the scenario following the tendency demonstrated by the data. In the case of Italy we obtain 8.61×10^6 and for France 1.23×10^7 . See Figs. 3(c) and 3(d). We are aware that such asymptotic behavior can be hardly trusted with numerical simulation of models. However, our intention in displaying such asymptotic behavior is to show that the proposed model converges to

reasonable values.

Now we discuss results for some emblematic scenarios for the model when strategies are applied to Italy and France on day March 28th. We can see that the strategy represented by the orange curves is not sufficient to significantly decrease the number of infected individual. Dark blue curves reduce the number of cases when compared to orange curves, but still increasing very much asymptotically. Light blue curves substantially decreases the asymptotic value, but still not satisfactory. A distinct behavior can be seen in the magenta continuous curve, which increases more sharply for around 10 days and then keeps a less accentuated increase for around 25 days. These local increases are due to the scenarios which identify infected individuals by testing them and, differently from the orange curve, both symptomatic and asymptomatic individuals are isolated. Thereby, these measures are able to substantially flatten the power-law growth. The same tendency is observed for black and green curves with smaller asymptotic value. Dashed curves for the strategies represented by colors magenta, green, and black, in this order, are the most efficient to flatten the curves and diminish the asymptotic values. Brown curves follow the light blue curve for Italy, and for France it is a bit lower than the light blue.

At next we discuss cases for Brazil and USA using other strategies. Results are shown in Figs. 4(a), 4(c) and Figs. 4(b), 4(d), respectively. Figures 4(c) and 4(d) furnish predictions for the number of infected individuals. Due to the distinct scenarios, we had to change a bit the color subtitles. Red curves: have the same meaning as before. Blue curves: still are related to the reduction of social interaction so that θ can take the values $\theta = 2.0, 1.5, 1.0$ and 0.5 , going from dark blue to light blue, until cyan color. Please see color labels in Fig. 4. Black curves: $\theta = 2.0$ and isolation of infected given by $\kappa_a = \kappa_s = 0.20$. Here we reduced the social interaction (when compared to the last value of θ^{eff}) and added the governmental intervention to isolate infected individuals. Grey curves: $\theta = 2.0$ and isolation of infected given by $\kappa_a = \kappa_s = 0.40$. Thus, in this case, we increase the daily ratio of identification and isolation of infected individuals (when compared to the strategy represented by the black curves). Dashed curves: parameters are the same as those from the continuous curves above, but represent the total number of confirmed symptomatic individuals. We notice that asymptomatic individuals, or those with very light symptoms, would not be identified without realization of tests and are not computed in the number of confirmed cases.

As in Fig. 3, during the times for which real data are available, the model chooses the values of the parameters θ and κ_s that better adjust the simulation results with

the real data. In the case of Brazil we obtain three values of θ^{eff} , as shown in Fig. 4(a) with the corresponding numerical values. In the case of USA we obtain just two values of θ^{eff} , as shown in Fig. 4(b) with the corresponding values. Red curves nicely fit the data as long they are available. For the USA case there were some difficult to adjust the parameters since the data show some irregularities. In the case for which the strategy does not change ($\theta = \theta^{eff}$ and $\kappa_s = \kappa_s^{eff}$), the red curves increase very much for both countries. Very high asymptotic values of infected individuals are reached.

Now we discuss results when governmental strategies are applied to Brazil and USA on March 28th. All blue curves (dark to cyan) tend to decrease the power-law inclination for both countries. However, values of $\theta = 2.0$ and 1.5 still lead to large asymptotic values. $\theta = 1.0$ leads to reasonable values and $\theta = 0.5$ is the most relevant strategy to flatten the curve efficiently. Surprisingly, black and gray curves have strong effects on the flattening, even though $\theta = 2.0$. As in Fig. 3, dashed curves are very efficient to flatten the curves of both countries.

IV. CONCLUSIONS

The power-law growth of the cumulative number of confirmed infected individuals by the COVID-19 until March 27th, 2020, is shown to be the best description

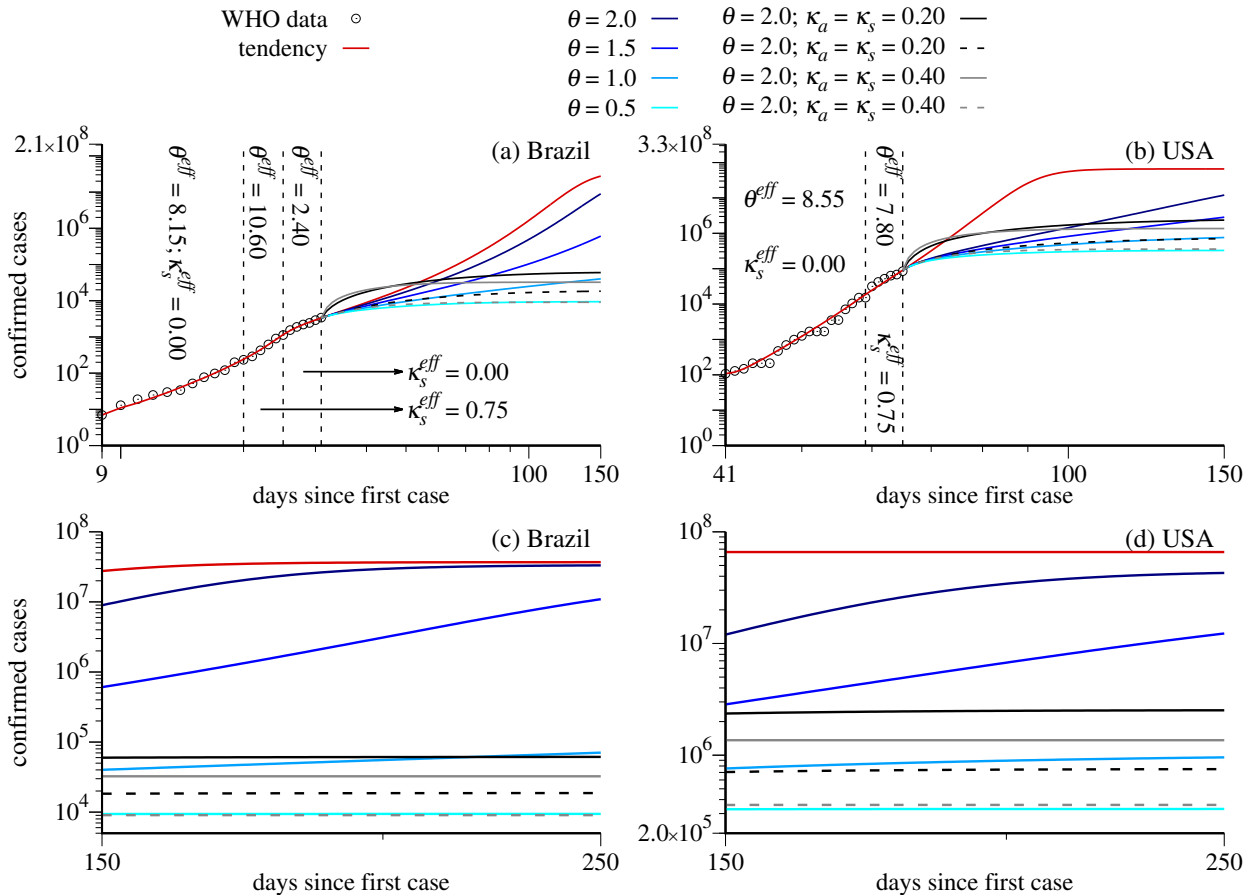


Figure 4. Log-log plot of cumulative number of confirmed cases (black circles) for Brazil [(a) and (c)] and USA [(b) and (d)] as a function of time and the projected number of cases (colored lines) using distinct governmental strategies (discussed in the text).

scenario for the countries: Brazil, China, France, Germany, Italy, Japan, Spain, Republic of Korea, and USA. Distinct power-law exponents for the countries are found and summarized in Table I. The power-law behavior suggests that the underlying propagation dynamics of the virus around the countries follows scale free networks, fractal kinetics and small world features [5, 6, 9]. While power-laws with distinct exponents may look similar visually, it is necessary to *quantify* this similarity. For this we compute the Distance Correlation [10–12] between all countries mentioned above (not shown). However, using representative countries of four continents, namely Brazil, Italy, Japan, and USA, results for the DC are presented in Fig. 2. They show that the power-law growth between these countries are highly correlated, even between north and south hemispheres. The high correlation between the power-law curves of different continents strongly suggest that government strategies can be applied with success around the whole World.

Furthermore, we propose a variation of the well known SEIR epidemic model [19, 20] for predictions using (or not) distinct governmental strategies applied on March 28th, 2020. We apply numerically distinct strategies to

flatten (or not) the power-law curves. Even though the social isolation, a well know benefit, is very powerful to flatten the curves, we found other strategies which lead to comparable results. We mention the specific scenario found for Brazil and USA for relative large values of social interaction ($\theta = 2.0$). An efficient flatten of the power-law is found in this case using $\kappa_a = \kappa_s = 0.2$, which means isolating 20% of the infected population *per* day, all the days. This can only be implemented in case of very strong government policies. It is crucial to mention that we are not computing the total of real infected cases, but only the confirmed ones. Being more specific, let us compare two scenarios in Brazil from Fig. 4(c), the cyan curve ($\theta = 0.5$ and $\kappa_a = \kappa_s = 0$) and the grey curve ($\theta = 2.0$ and $\kappa_a = \kappa_s = 0.4$). While the scenario represented by the cyan curve predicts approximately 9500 confirmed cases of a total of around 47000, the scenario represented by the grey curve predicts approximately 32000 confirmed cases of a total of around 45000. Therefore, the strategy of identifying and isolating infected cases is more relevant than the social isolation, since its number of total cases is smaller. In addition, high level of isolation is needed to obtain the cyan

curve scenario. The above combination between social interaction and the degree of isolation of infected individuals can be essential to prevent economic catastrophes because people are not working. In other words, let some essential individuals go back to work (increasing θ) and, *simultaneously*, increase by a huge amount the number of tests and isolation of infected individuals. This furnishes an efficient scenario to flatten the power-law.

V. APPENDIX A - THE DISTANCE CORRELATION

In this section we give a precise definition of the DC following [10]. Consider joint random sample $(\mathbf{X}, \mathbf{Y}) = \{(X_k, Y_k) : k = 1, \dots, N\}$ with $X, Y \in \mathbb{R}^p$ and $N \geq 2$, with $i = 1, \dots, N$ and $j = 1, \dots, N$. In addition consider the matrix $A_{ij} = a_{ij} - \bar{a}_i - \bar{a}_j + \bar{a}_{..}$, where $a_{ij} = |X_i - X_j|_p$ is the Euclidean norm of the distance between the elements of the sample, $\bar{a}_i = \frac{1}{N} \sum_{j=1}^N a_{ij}$ and $\bar{a}_j = \frac{1}{N} \sum_{i=1}^N a_{ij}$ are the arithmetic mean of the rows and columns, respectively, and $\bar{a}_{..} = \frac{1}{N^2} \sum_{i,j=1}^N a_{ij}$ is the general mean. A similar matrix $B_{ij} = b_{ij} - \bar{b}_i - \bar{b}_j + \bar{b}_{..}$, can be defined using $b_{ij} = |Y_i - Y_j|_p$. The terms b_{ij} , \bar{b}_i , \bar{b}_j and $\bar{b}_{..}$ are similar to those from matrix A_{ij} . From these matrices we compute the *empirical distance correlation* from

$$DC_N(\mathbf{X}, \mathbf{Y}) = \frac{\sigma_N(\mathbf{X}, \mathbf{Y})}{\sqrt{\sigma_N(\mathbf{X})\sigma_N(\mathbf{Y})}}, \quad (1)$$

where

$$\sigma_N(\mathbf{X}, \mathbf{Y}) = \frac{1}{N} \sqrt{\sum_{i,j=1}^N A_{ij} B_{ij}}, \quad (2)$$

and

$$\sigma_N(\mathbf{X}) = \frac{1}{N} \sqrt{\sum_{i,j=1}^N A_{ij}^2}, \quad \sigma_N(\mathbf{Y}) = \frac{1}{N} \sqrt{\sum_{i,j=1}^N B_{ij}^2}. \quad (3)$$

VI. APPENDIX B - THE MODEL

The proposed model contains six ODEs and is an extension of a model known in the literature [21, 22]. Many other related models have been proposed with distinct characteristics [21–26]. In our case we consider symptomatic I_s and asymptomatic I_a infected individuals. Quarantine Q is also contemplated, respectively. The transition rate from asymptomatic to symptomatic cases is neglected as an first approach. The Ordinary Differen-

tial Equations (ODEs) are given by

$$\dot{S} = -\frac{\theta}{T_{inf}} \frac{(I_s + \alpha I_a)}{N} S, \quad (4)$$

$$\dot{E} = \frac{\theta}{T_{inf}} \frac{(I_s + \alpha I_a)}{N} S - \frac{E}{T_{lat}}, \quad (5)$$

$$\dot{I}_s = (1 - \beta) \frac{E}{T_{lat}} - \left(\kappa_s + \frac{1}{T_{inf}} \right) I_s, \quad (6)$$

$$\dot{I}_a = \beta \frac{E}{T_{lat}} - \left(\kappa_a + \frac{1}{T_{inf}} \right) I_a, \quad (7)$$

$$\dot{Q} = \kappa_s I_s + \kappa_a I_a - \frac{Q}{T_{inf}}, \quad (8)$$

$$\dot{R} = \frac{1}{T_{inf}} (I_s + I_a + Q). \quad (9)$$

The dot represents the time derivative and the variables are:

- $N = S + E + I_s + I_a + Q + R$: total population.
- S : individuals susceptible to infection.
- E : exposed individuals, remain latent until infected.
- I_s : symptomatic individuals.
- I_a : asymptomatic individuals.
- Q : infected individuals isolated (in quarantine),
- R : individuals which were infected and not identified but became immune.

To adjust the parameters following distinct countries, as well as government measures, we used the cumulative number of confirmed infected individuals C_{cum} . The number of confirmed infected individuals as a function of time is defined by $C(t) = I_s(t) + Q(t)$. Parameters which do not depend on strategies are:

- $T_{inf} = 8$ days: time interval the infected individual remains infected.
- $T_{lat} = 5$ days: time interval the exposed individual keeps not infected, also denominated incubation time.
- $\alpha = 1.0$: ratio between infectiousness of asymptomatic and symptomatic individuals.
- $\beta = 0.8$: population ratio which remains asymptomatic.

Parameters which are related to the use of distinct strategies are:

- $\theta = \gamma R_0$: replication factor, with γ being a number that represents the proportion of interaction between individuals and R_0 the basic reproduction number. In our model, θ is an adjustable parameter according to WHO data.

- κ_s : identification rate of symptomatic individuals, which are then putted into quarantine.
- κ_a : identification rate of asymptomatic individuals, which are then putted in quarantine.

In this model, no rigid quarantine is taken into account and no immunization term is defined, since until today no vaccine has been developed. In Eq. (8), the factor T_{inf} dividing Q represents a rate of exit from the quarantine (for the group R), which is equal to the natural development of the disease. This is an approximation since the correct way would be to have an isolation time which could be smaller than T_{inf} , then symptomatic individuals do not transit instantaneously to quarantine. By considering this exit rate to isolation we change the balance between the confirmed cases and the asymptomatic ones. This proportional break is not accentuated but can be observed in the time-series in the refereed specific groups, namely susceptible, infectious, exposed, etc.

It is important to mention that the parameters θ and κ_s are adjusted together with the variable E . The goal is to minimize the mean square error between the predicted curve and real data. Parameter κ_a is only adjusted when there are information available about the test realization in the population. We do not start the parameter's adjustment from the first day of reported infections, but later on. The model produces better results in such cases.

The initial condition set used in the numerical integration process of the ODEs is the following: $Q(t_0) = R(t_0) = 0$; $I_a(t_0) = \beta I_s(t_0)/(1 - \beta)$, where $I_s(t_0)$ represent the number of confirmed infected cases, obtained from the real time-series for the day t_0 . $S(t)$ is determined accordingly to the total number of people for each country and the previous initial conditions.

ACKNOWLEDGMENTS

The authors thank CNPq (Brazil) for financial support (grant numbers 432029/2016-8, 304918/2017-2, 310792/2018-5 and 424803/2018-6) and, they also acknowledge computational support from Prof. C. M. de Carvalho at LFTC-DFis-UFPR (Brazil). C. M. also thanks FAPESC (Brazilian agency) for financial support and Luiz A. F. Coelho and Joel M. Crichigno Filho for fruitful discussions.

DATA AVAILABILITY

The data that support the findings of this study are openly available in WHO (World Health Organization), situation reports 1–68 [13].

-
- [1] T. Puevo, “Coronavirus: Why you must act now,” <https://medium.com/@tomaspuero/coronavirus-act-today-or-people-will-die-f4d3d9cd99c> (2020).
- [2] A. Vazquez, “Polynomial growth in branching processes with diverging reproductive number,” *Phys. Rev. E* **96**, 038702 (2006).
- [3] H. W. Hethcote, “The mathematics of infectious diseases,” *SIAM Review* **42**, 599–653 (2000).
- [4] G. M. Viswanathan, M. G. E. da Luz, E. P. Raposo, and H. E. Stanley, *The physics of foraging: an introduction to random searches and biological encounters* (Cambridge University Press, 2011).
- [5] D. J. Watts, *Small worlds: the dynamics of networks between order and randomness* (Princeton University Press, 2004).
- [6] T. Ray, “Graph theory suggests COVID-19 might be a ‘small world’ after all,” <https://www.zdnet.com/article/graph-theory-suggests-covid-19-might-be-a-small-world-after-all/> (2020).
- [7] H. M. Singer, “Short-term predictions of country-specific COVID-19 infection rates based on power law scaling exponents,” arXiv:2003.11997v1 (2020).
- [8] B. F. Maier and D. Brockmann, “Effective containment explains sub-exponential growth in confirmed cases of recent COVID-19 outbreak in Mainland China,” arXiv:2002.07572v1 (2020).
- [9] A. Ziff and R. Ziff, “Fractal kinetics of COVID-19 pandemic,” <https://doi.org/10.1101/2020.02.16.20023820> (2020).
- [10] G. J. Székely, M. L. Rizzo, and N. K. Bakirov, “Measuring and testing dependence by correlation of distances,” *Ann. Statist.* **35**, 2769–2794 (2007).
- [11] C. F. O. Mendes and M. W. Beims, “Distance correlation detecting Lyapunov instabilities, noise-induced escape times and mixing,” *Physica A* **512**, 721–730 (2018).
- [12] C. F. O. Mendes, R. M. da Silva, and M. W. Beims, “Decay of the distance autocorrelation and Lyapunov exponents,” *Phys. Rev. E* **99**, 062206 (2019).
- [13] World Health Organization, “Coronavirus disease (COVID-2019) situation reports,” <https://www.who.int/emergencies/diseases/novel-coronavirus-2019/situation-reports/> (2020).
- [14] PreventionWeb, “How South Korea is suppressing COVID-19,” <https://www.preventionweb.net/news/view/71028> (2020).
- [15] G. J. Székely and M. L. Rizzo, “Brownian distance covariance,” *Ann. Appl. Stat.* **3**, 1236–1265 (2009).
- [16] G. J. Székely and M. L. Rizzo, “On the uniqueness of distance covariance,” *Stat. Probabil. Lett.* **82**, 2278–2282 (2012).
- [17] G. J. Székely and M. L. Rizzo, “The distance correlation t-test of independence in high dimension,” *J. Multivariate Anal.* **117**, 193–213 (2013).
- [18] G. J. Székely and M. L. Rizzo, “Partial distance correlation with methods for dissimilarities,” *Ann. Stat.* **42**, (2020).

- 2382–2412 (2014).
- [19] M. Y. Li, J. R. Graef, L. Wang, and J. Karsai, “Global dynamics of a SEIR model with varying total population size,” *Math. Biosci.* **160**, 191 – 213 (1999).
- [20] J. T. Wu, K. Leung, and G. M. Leung, “Nowcasting and forecasting the potential domestic and international spread of the 2019-nCoV outbreak originating in Wuhan, China: a modelling study,” *The Lancet* **395**, 689 – 697 (2020).
- [21] K. M. Khalil, M. Abdel-Aziz, T. T. Nazmy, and A. B. M. Salem, “An agent-based modeling for pandemic influenza in Egypt,” in *Handbook on Decision Making* (Springer, 2012) pp. 205–218.
- [22] B. J. Coburn, B. G. Wagner, and S. Blower, “Modeling influenza epidemics and pandemics: insights into the future of swine flu (H1N1),” *BMC Med.* **7**, 30 (2009).
- [23] B. F. Maier and D. Brockmann, “Effective containment explains sub-exponential growth in confirmed cases of recent COVID-19 outbreak in Mainland China,” arXiv preprint arXiv:2002.07572 (2020).
- [24] Y. S. Long, Z. M. Zhai, L. L. Han, J. Kang, Y. L. Li, Z. H. Lin, L. Zeng, D. Y. Wu, C. Q. Hao, M. Tang, Z. Liu, and Y. C. Lai, “Quantitative assessment of the role of undocumented infection in the 2019 novel coronavirus (COVID-19) pandemic,” arXiv preprint arXiv:2003.12028 (2020).
- [25] H. Hethcote, M. Zhién, and L. Shengbing, “Effects of quarantine in six endemic models for infectious diseases,” *Math. Biosci.* **180**, 141 – 160 (2002).
- [26] Q. Li, X. Guan, P. Wu, X. Wang, L. Zhou, Y. Tong, R. Ren, K. S. M. Leung, E. H. Y. Lau, J. Y. Wong, *et al.*, “Early transmission dynamics in Wuhan, China, of novel coronavirus-infected pneumonia,” *N. Engl. J. Med.* **382**, 1199–1207 (2020).